

AD-A148 076

ELECTROMAGNETIC FIELDS FROM THE GENERATION AND  
ABSORPTION OF DISCONTINUOUS LINEAR CURRENT FRONTS(U)  
MEGAPULSE INC BEDFORD MASS E A LEWIS JUL 84

1/1

UNCLASSIFIED

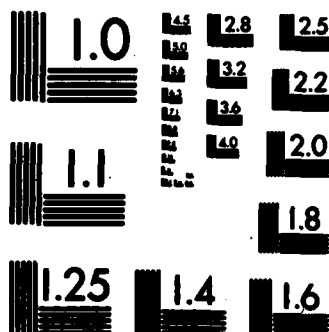
RADC-TR-84-153 F19628-80-C-0146

F/G 28/3

NL

END

FILED



MICROCOPY RESOLUTION TEST CHART  
NATIONAL BUREAU OF STANDARDS-1963-A

**RADC-TR-84-153**

**Interim Report**

**June 1984**

*July*



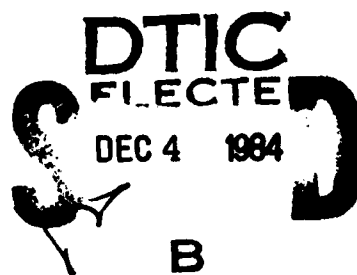
12

# ***ELECTROMAGNETIC FIELDS FROM THE GENERATION AND ABSORPTION OF DISCONTINUOUS LINEAR CURRENT FRONTS***

**Megapulse, Inc.**

**Dr. Edward A. Lewis**

**APPROVED FOR PUBLIC RELEASE; DISTRIBUTION UNLIMITED**



**ROME AIR DEVELOPMENT CENTER  
Air Force Systems Command  
Griffiss Air Force Base, NY 13441**

**84 11 28 004**

AD-A148 076

DTIC FILE COPY

This report has been reviewed by the RADC Public Affairs Office (PA) and is releasable to the National Technical Information Service (NTIS). At NTIS it will be releasable to the general public, including foreign nations.

RADC-TR-84-153 has been reviewed and is approved for publication.

APPROVED: *Wayne I. Klemetti*

WAYNE I. KLEMETTI  
Project Engineer

APPROVED: *Allan C. Schell*

ALLAN C. SCHELL  
Chief, Electromagnetic Sciences Division

FOR THE COMMANDER:

*John A. Ritz*

JOHN A. RITZ  
Acting Chief, Plans Office

If your address has changed or if you wish to be removed from the RADC mailing list, or if the addressee is no longer employed by your organization, please notify RADC (EEPS) Hanscom AFB MA 01731. This will assist us in maintaining a current mailing list.

Do not return copies of this report unless contractual obligations or notices on a specific document requires that it be returned.

UNCLASSIFIED

SECURITY CLASSIFICATION OF THIS PAGE

## REPORT DOCUMENTATION PAGE

1a. REPORT SECURITY CLASSIFICATION <b>UNCLASSIFIED</b>		1b. RESTRICTIVE MARKINGS <b>N/A</b>	
2a. SECURITY CLASSIFICATION AUTHORITY <b>N/A</b>		3. DISTRIBUTION/AVAILABILITY OF REPORT Approved for public release; distribution unlimited	
2b. DECLASSIFICATION/DOWNGRADING SCHEDULE <b>N/A</b>		5. MONITORING ORGANIZATION REPORT NUMBER(S) <b>RADC-TR-84-153</b>	
4. PERFORMING ORGANIZATION REPORT NUMBER(S) <b>N/A</b>		7a. NAME OF MONITORING ORGANIZATION <b>Rome Air Development Center (EEPS)</b>	
6a. NAME OF PERFORMING ORGANIZATION <b>Megapulse, Inc.</b>	6b. OFFICE SYMBOL (If applicable)	7b. ADDRESS (City, State and ZIP Code) <b>Hanscom AFB MA 01731</b>	
6c. ADDRESS (City, State and ZIP Code) <b>8 Preston Court Bedford MA 01730</b>		8. PROCUREMENT INSTRUMENT IDENTIFICATION NUMBER <b>F19628-80-C-0146</b>	
8a. NAME OF FUNDING/SPONSORING ORGANIZATION <b>Rome Air Development Center</b>	8b. OFFICE SYMBOL (If applicable) <b>EEPS</b>	10. SOURCE OF FUNDING NOS.	
8c. ADDRESS (City, State and ZIP Code) <b>Hanscom AFB MA 01731</b>		PROGRAM ELEMENT NO. <b>62702F</b>	PROJECT NO. <b>4600</b>
		TASK NO. <b>16</b>	WORK UNIT NO. <b>44</b>
11. TITLE (Include Security Classification) <b>ELECTROMAGNETIC FIELDS FROM THE GENERATION AND ABSORPTION OF DISCONTINUOUS LINEAR CURRENT FRONTS</b>			
12. PERSONAL AUTHOR(S) <b>Dr. Edward A. Lewis</b>			
13a. TYPE OF REPORT <b>Interim</b>	13b. TIME COVERED <b>FROM 1May82 to 1May83</b>	14. DATE OF REPORT (Yr., Mo., Day) <b>July 1984</b>	15. PAGE COUNT <b>42</b>
16. SUPPLEMENTARY NOTATION <b>N/A</b>			
17. COSATI CODES		18. SUBJECT TERMS (Continue on reverse if necessary and identify by block number)	
FIELD	GROUP	SUB. GR.	
<b>20</b>	<b>14</b>		
		<b>Electromagnetic potentials</b>	
		<b>Electromagnetic fields</b>	
		<b>Discontinuous linear current</b>	
19. ABSTRACT (Continue on reverse if necessary and identify by block number) The relativistically correct potentials and fields are calculated for a basic electromagnetic source-model in which the electric charge at a fixed point suddenly starts increasing linearly with time, while the equal but opposite charge flows away from the point with constant velocity in a straight line. A numerical example of a field calculation is given. Limiting forms of the solution appropriate at great distances are found, and radiated power, radiation resistance, and radiation patterns are derived. Using the solution for this basic model, solutions for other source-models are developed by linear superposition. These include fields from a current being generated at one point and stopped (absorbed) at another, and the fields from current impulses.			
20. DISTRIBUTION/AVAILABILITY OF ABSTRACT <b>UNCLASSIFIED/UNLIMITED</b> <input checked="" type="checkbox"/> SAME AS RPT. <input type="checkbox"/> DTIC USERS <input type="checkbox"/>		21. ABSTRACT SECURITY CLASSIFICATION <b>UNCLASSIFIED</b>	
22a. NAME OF RESPONSIBLE INDIVIDUAL <b>Wayne I. Klemetti</b>		22b. TELEPHONE NUMBER (Include Area Code) <b>617-861-4329</b>	22c. OFFICE SYMBOL <b>RADC (EEPS)</b>

# TABLE OF CONTENTS

<u>Section No.</u>		<u>Page No.</u>
ABSTRACT		111
1	Introduction .....	1
2	Retarded Potentials for the Current-Generation .....	1
3	Exact Fields for the Current-Generation .....	5
4	Limiting Forms for Large Distances and Early Times .	14
5	Numerical Example .....	22
6	Exact Solution with Current-Absorption .....	24
7	Limiting Forms with Current-Absorption .....	29
Appendix A	Inversion of Time-Distance Equation .....	32
	References .....	33

## LIST OF FIGURES

<u>Figure No.</u>		<u>Page No.</u>
2.1	COORDINATES IN THE PLANE CONTAINING THE LINE-CHARGE (OZ axis) AND THE OBSERVATION POINT, P .....	2
3.1	RELATION OF ELECTRIC FIELD-COMPONENTS IN CYLINDRICAL AND SPHERICAL COORDINATE SYSTEMS .....	12
4.1	DIRECTIVITY PATTERNS FOR EARLY TIMES .....	16
4.2	CROSSECTION OF THE SPACE BETWEEN TWO NEIGHBORING WAVEFRONTS .....	18
4.3	ELEMENT OF INTEGRATION .....	20
4.4	GRAPH OF THE FUNCTION $B(\beta)$ .....	21
5.1	GROWTH OF MAGNETIC FIELD $H_\phi$ FROM EQUATION 5.6 .....	25
5.2	GROWTH OF THE ELECTRIC FIELD COMPONENT $E_r$ FROM EQUATION 5.9 .....	26
5.3	GROWTH OF THE ELECTRIC FIELD COMPONENT $E_z$ OF EQUATION 5.12 .....	27
6.1	VERSION OF FIGURE 2.1 FOR THE CASE WHEN THE UPWARD - ADVANCING CURRENT-FRONT IS ABSORBED AT $z = L$ .....	28

TABLE OF CONTENTS  
(continued)

LIST OF FIGURES

<u>Figure No.</u>		<u>Page No.</u>
7.1	GENERATING AND ABSORBING A CURRENT IMPULSE GIVES A DOUBLE-IMPULSE RADIATION FIELD .....	30
7.2	SYNTHESIS OF RADIATION FIELD FROM GENERATING AND ABSORBING AN ARBITRARY CURRENT .....	31

DTIC  
ELECTE  
DEC 4 1984  
S D  
B



Accession For	
NTIS GRA&I	<input checked="" type="checkbox"/>
DTIC TAB	<input type="checkbox"/>
Unannounced	<input type="checkbox"/>
Justification	
PER CALL JC	
By	
Distribution/	
Availability Codes	
Dist	Avail and/or Special
A-1	

## 1. INTRODUCTION

In this paper the electromagnetic fields are calculated for a basic source-model in which an unspecified charge-separation process results in the linear build-up of charge at a fixed point, while an equal but opposite charge flows away from the point with constant velocity in a straight line. This model might apply to the case of a free-space ion-gun, which when suddenly switched on, produces a beam of current while charge builds up on the gun. The model assumes a current in the form of a step-function thus providing the basis for treating more complicated current variations by linear superposition methods. For example, the fields from the time-varying current wave which is excited by a corona discharge at the end of a long straight conductor might be synthesized in this way.

Whereas some aspects of a similar but less general problem have already been treated,<sup>1</sup> the present work develops the complete solution for arbitrary observation distances, directions and times. In addition Sections 6, 7, and 8 consider the fields caused by generating the current at one point, and stopping (absorbing) it at another. This process creates a charge dipole of finite length and varying moment.

## 2. RETARDED POTENTIALS FOR THE CURRENT-GENERATION

Figure 2.1 illustrates a cylindrical coordinate system in which the observation point P has the coordinates  $r, z, \phi$ , the  $\phi$ -direction being into the plane of the figure. The charge separation process is localized at the origin O, and starts at time  $t = 0$ . This process feeds charge at a constant rate into the line represented by the positive Z-axis, and the charge moves at constant velocity  $v$  in the form of an advancing step-function of charge density  $\rho$  coul/m. The moving charge is equivalent to a current behind the front.

$$J = v\rho \quad (2.1)$$

An equal but opposite charge

$$q = -Jt \quad (2.2)$$

builds up at the origin and remains there.

With all charges and currents confined to one dimension (Z-axis) the volume integrals of the general expressions for the retarded potentials<sup>2</sup> reduce immediately to single integrals. Also because of symmetry with respect to  $\phi$ , there is only one component of the magnetic vector potential  $\bar{A}$ , namely

$$A_z(r, z; t) = \frac{\mu_0}{4\pi} \int_{-\infty}^{\infty} \frac{J(z_1, \tau)}{R_1} dz_1 \quad (\text{MKS}) \quad (2.3)$$

Here

$$R_1 = \sqrt{(z - z_1)^2 + r^2} \quad (2.4)$$

<sup>1</sup> Lewis, E.A., "Radiation from Idealized Shock Excitation Currents in a Straight Conductor Rising from a Perfect Earth at an Arbitrary Angle" Electromagnetic Wave Propagation, Academic Press, 1958, p335.

<sup>2</sup> Stratton, J.A. Electromagnetic Theory, McGraw-Hill, 1941.



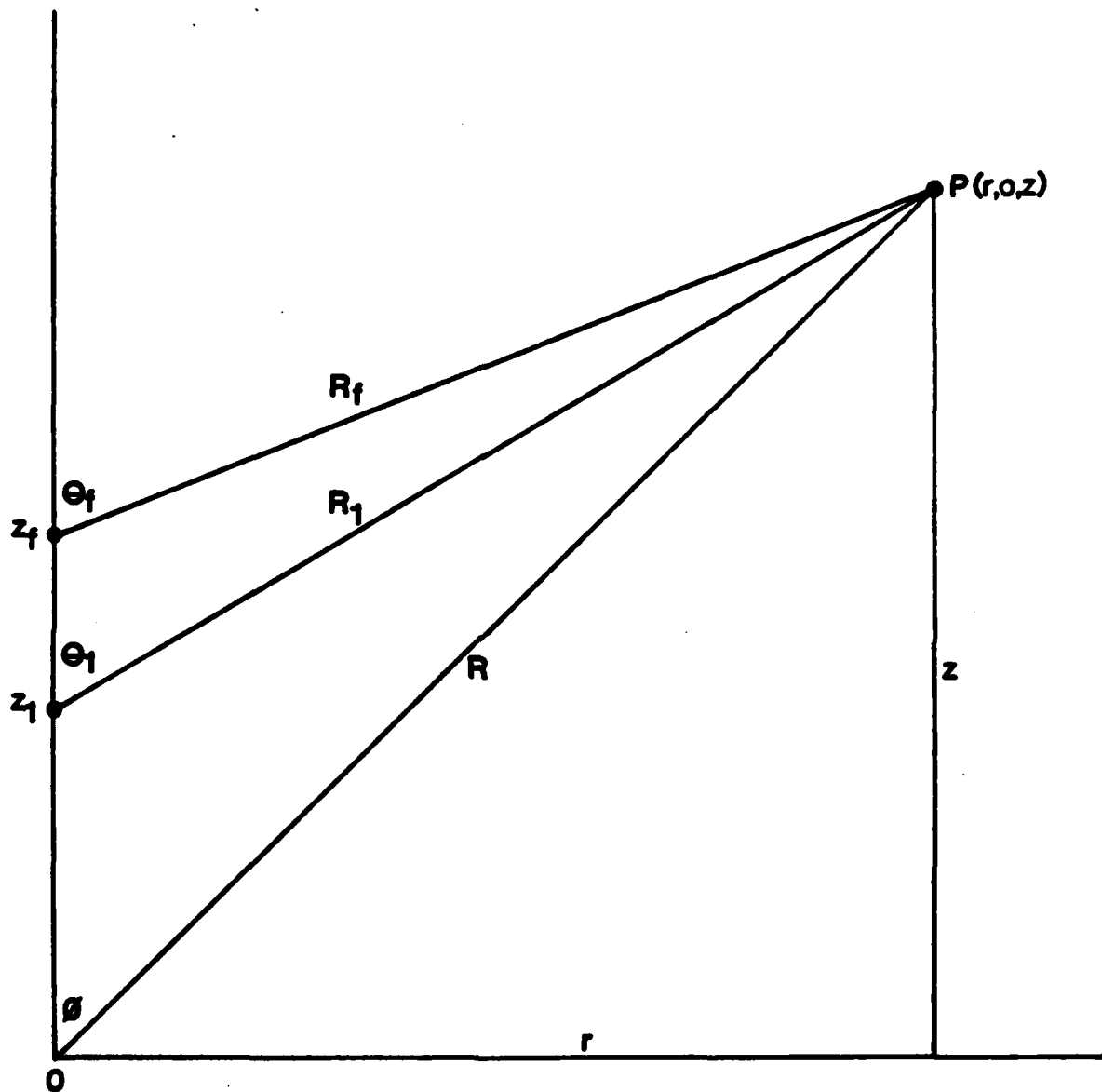


Figure 2.1

Coordinates in the Plane Containing the Line-Charge and the Observation Point,  $P$

$$R = \sqrt{z^2 + r^2} \quad (2.5)$$

and the current  $J$  at point  $P$  is to be evaluated at the "retarded time"

$$\tau = t - R_1/c \quad (2.6)$$

In the integrand,  $J$  is zero for  $t$  less than  $R/c$ , and so also is  $A_z$ .

The retarded time  $\tau$  is the time a wavelet travelling with free-space velocity  $c$ , would have to leave the element of integration  $dz$ , at  $z = z_1$ , in order to arrive at point  $P$  at time  $t$ . At the moment when the front edge of the step-function has reached the point  $z = z_f$ , a time  $z_f/V$  has already elapsed. The first contribution from the element at  $z_f$  does not reach the observer at  $P$  until after a further time-interval  $R_f/c$  where

$$R_f = \sqrt{(z - z_f)^2 + r^2} = \sqrt{R^2 - 2zz_f + z_f^2} \quad (2.7)$$

see Figure 2.1. Thus the arrival time of the first wavelet from the element at  $z_f$  is

$$t = \frac{z_f}{v} + \frac{1}{c} \sqrt{(z - z_f)^2 + r^2} \quad (2.8)$$

This "time-distance" equation can be solved to give  $z_f$  as a closed-form function of  $r$ ,  $z$ , and  $t$ , see Appendix A. The resulting expression is rather cumbersome, and it happens that the inversion process can often be avoided, especially in numerical work. The main features of the solution may be understood by noting in Figure 2.1 that if  $R \gg z_f$ ,

$$R_f \approx R - z_f \cos \theta \quad (2.9)$$

and

$$t \approx \frac{z_f}{v} + \frac{R}{c} - \frac{z_f}{c} \cos \theta \quad (2.10)$$

that is

$$z_f \approx \frac{v(t - R/c)}{1 - \beta \cos \theta} \quad (2.11)$$

where  $\beta = b/c$ . If  $\beta \approx 1$  and if  $\theta \approx 0^\circ$ , the denominator is small, and  $z_f$  can be correspondingly large.

With the same notation, the scalar potential, see Stratton,<sup>2</sup> is

$$\phi(r, z; t) = \frac{1}{4\pi\epsilon_0} \int_{-\infty}^{\infty} \frac{\rho(z_1; \tau)}{R_1} dz_1 \quad (t > R/c) \quad (2.12)$$

For convenience this integral will be considered to have two parts:

$$\phi = \phi_m + \phi_s, \quad (2.13)$$

where  $\phi_m$  is due to the moving charge, and  $\phi_s$  is due to the time-varying, but stationary charge at the origin. Then

$$\phi_m = \frac{1}{4\pi\epsilon_0} \int_{0+}^{\infty} \frac{\rho(z_1; \tau)}{R_1} dz_1 \quad (2.14)$$

where the lower bound of integration excludes the origin. The integration over the stationary charge at the origin is a degenerate one, giving immediately

$$\begin{aligned} \phi_s &= \frac{1}{4\pi\epsilon_0} \cdot q(\tau) \\ &= - \frac{J \cdot (t - R/c)}{4\pi\epsilon_0 R} \end{aligned} \quad (2.15)$$

on using Equation 2.2.

For a given set of values  $(r, z, t)$  there is no contribution to the integrals for  $A_z$  and  $\phi_m$  from those elements for which  $z^1 > z_f$  and there is never any contribution from elements with negative values of  $z$ . Also, within the range  $0 < z_1 < z_f$ ,  $\rho$  and  $J$  are constant, so that

$$A_z(r, z; t) = \frac{\mu_0 J}{4\pi} I \quad (2.16)$$

and

$$\phi_m(r, z; t) = \frac{J}{4\pi\epsilon_0 v} I \quad (2.17)$$

where

$$I = \int_0^{z_f} \frac{dz_1}{\sqrt{(z-z_1)^2 + r^2}} \quad (2.18)$$

On setting

$$\xi = z - z_1 \quad (2.19)$$

$$I = \int_{z-z_f}^z \frac{d\xi}{\sqrt{\xi^2 + r^2}} \quad (2.20)$$

$$= \left[ \ln \left( \xi + \sqrt{\xi^2 + r^2} \right) \right]_{z-z_f}^z \quad (2.21)$$

as may be verified by differentiation. Thus,

$$I = \ln \left( z + \sqrt{z^2 + r^2} \right) - \ln \left( z - z_f + \sqrt{(z-z_f)^2 + r^2} \right) \quad (2.22)$$

This provides the formal solution for the retarded potentials in exact closed form. The next section discusses the derivation of the fields from the potentials - a procedure in which it must be remembered that  $z_f$  contains  $r$ ,  $z$ , and  $t$  through the time-distance equation (Equation 2.8).

### 3. EXACT FIELDS FOR THE CURRENT-GENERATION

The electric and magnetic fields are to be obtained from the potentials by means of the standard vector operators:

$$\vec{E} = -\nabla\phi - \frac{\partial \vec{A}}{\partial t} \quad (3.1)$$

$$\vec{H} = \frac{1}{\mu_0} \nabla \times \vec{A} \quad (3.2)$$

In cylindrical coordinates with the present axial symmetry (no dependence on  $\phi$ ) there are only three basic field components:

$$H_{\phi} = -\frac{1}{\mu_0} \frac{\partial A_z}{\partial r} \quad (3.3)$$

$$E_z = -\frac{\partial \phi}{\partial z} - \frac{\partial A_z}{\partial t} \quad (3.4)$$

$$E_r = -\frac{\partial \phi}{\partial r} \quad (3.5)$$

Each of the above electric field components can be regarded as being the sum of contributions from the moving and stationary charges. Denoting these by subscripts  $m$  and  $s$  respectively,

$$E_z = E_{zm} + E_{zs} \quad (3.6)$$

$$E_r = E_{rm} + E_{rs} \quad (3.7)$$

Remembering that  $\phi$  also has two parts, see Equation 2.13, it is evident from Equation 3.4 that

$$E_{zm} = -\frac{\partial \phi_m}{\partial z} - \frac{\partial A_z}{\partial t} \quad (3.8)$$

and

$$E_{zs} = -\frac{\partial \phi_s}{\partial z} \quad (3.9)$$

Similarly, from Equation 3.5,

$$E_{rm} = -\frac{\partial \phi_m}{\partial r} \quad (3.10)$$

$$E_{rs} = -\frac{\partial \phi_s}{\partial r} \quad (3.11)$$

Since by Equation 2.15,

$$\phi_s = -\frac{Jt}{4\pi\epsilon_0 R} + \frac{J}{4\pi\epsilon_0 C} ,$$

$$\frac{\partial\phi_s}{\partial z} = \frac{\partial\phi_s}{\partial R} \cdot \frac{\partial R}{\partial z} = \frac{Jt}{4\pi\epsilon_0 R^2} \cdot \frac{\partial R}{\partial z} , \quad (3.12)$$

and

$$\frac{\partial\phi_s}{\partial r} = \frac{\partial\phi_s}{\partial R} \cdot \frac{\partial R}{\partial r} = \frac{Jt}{4\pi\epsilon_0 R^2} \cdot \frac{\partial R}{\partial r} . \quad (3.13)$$

On differentiating Equation 2.5, and referring to Figure 2.1,

$$\frac{\partial R}{\partial z} = \frac{z}{R} = \cos\theta \quad (3.14)$$

$$\frac{\partial R}{\partial r} = \frac{r}{R} = \sin\theta \quad (3.15)$$

Then

$$E_{zs} = -\frac{Jt}{4\pi\epsilon_0} \cdot \frac{\cos\theta}{R^2} , \quad (t > R/c) \quad (3.16)$$

and

$$E_{rs} = -\frac{Jt}{4\pi\epsilon_0} \cdot \frac{\sin\theta}{R^2} . \quad (t > R/c) \quad (3.17)$$

Referring to Equations 2.16 and 2.17, Equation 3.8 gives

$$E_{zm} = -\frac{J}{4\pi\epsilon_0 v} \left( \frac{\partial I}{\partial z} + \mu\epsilon_0 v \frac{\partial I}{\partial t} \right) , \quad (3.18)$$

while by Equation 3.10,

$$E_{rm} = -\frac{J}{4\pi\epsilon_0 v} \cdot \frac{\partial I}{\partial r} . \quad (3.19)$$

Similarly, Equation 3.3 becomes

$$H_{\phi} = -\frac{J}{4\pi} \cdot \frac{\partial I}{\partial r} \quad (3.20)$$

On writing  $\beta = v/c$ , and  $Z_0 = \sqrt{\frac{\mu_0}{\epsilon_0}} = \frac{1}{\epsilon_0 c}$ ,

$$H_{\phi} = \frac{\beta}{Z_0} E_{rm} \quad (3.21)$$

It remains to develop expressions for the partial derivatives of  $I$ . Noting from Figure 2.1 that

$$\frac{z - z_f}{R_f} = \cos\theta_f, \quad (3.22)$$

and

$$\frac{r}{R_f} = \sin\theta_f, \quad (3.23)$$

differentiating Equation 2.22 with respect to  $r$  gives

$$\begin{aligned} \frac{\partial I}{\partial r} &= \frac{\frac{r}{\sqrt{z^2 + r^2}}}{z + \sqrt{z^2 + r^2}} - \frac{-\frac{\partial z_f}{\partial r} + \frac{-(z-z_f)}{\sqrt{(z-z_f)^2 + r^2}} + r}{z - z_f + \sqrt{(z-z_f)^2 + r^2}} \\ &= \frac{\sin\theta}{R(1+\cos\theta)} + \frac{\frac{\partial z_f}{\partial r} + \cos\theta_f \frac{\partial z_f}{\partial r} - \sin\theta_f}{R_f(1+\cos\theta_f)} \\ &= \frac{\sin\theta}{R(1+\cos\theta)} - \frac{\sin\theta_f}{R_f(1+\cos\theta_f)} + \frac{1}{R_f} \frac{\partial z_f}{\partial r} \end{aligned} \quad (3.24)$$

Similarly,

$$\begin{aligned}
 \frac{\partial I}{\partial t} &= - \frac{-\frac{\partial z_f}{\partial t} - \frac{(z-z_f) \frac{\partial z_f}{\partial t}}{\sqrt{(z-z_f)^2 + r^2}}}{z - z_f + \sqrt{(z-z_f)^2 + r^2}} \\
 &= \frac{1 + \cos \theta_f}{R_f (1 + \cos \theta_f)} \frac{\partial z_f}{\partial t} \\
 &= \frac{1}{R_f} \frac{\partial z_f}{\partial t} \quad . \quad (3.25)
 \end{aligned}$$

Also

$$\begin{aligned}
 \frac{\partial I}{\partial z} &= \frac{1 + \frac{z}{\sqrt{z^2 + r^2}}}{z + \sqrt{z^2 + r^2}} - \frac{1 - \frac{\partial z_f}{\partial z} + \frac{(z-z_f) \left(1 - \frac{\partial z_f}{\partial z}\right)}{\sqrt{(z-z_f)^2 + r^2}}}{(z-z_f) + \sqrt{(z-z_f)^2 + r^2}} \\
 &= \frac{1}{R} - \frac{1}{R_f} \left(1 - \frac{\partial z_f}{\partial z}\right) \quad (3.26)
 \end{aligned}$$

On differentiating the time-distance equation (Equation 28) with respect to  $r$ ,

$$\begin{aligned}
 0 &= \frac{1}{v} \frac{\partial z_f}{\partial r} + \frac{1}{c} \frac{(z-z_f) \left(-\frac{\partial z_f}{\partial r}\right) + r}{\sqrt{(z-z_f)^2 + r^2}} \\
 &= \frac{1}{v} \frac{\partial z_f}{\partial r} - \frac{\cos \theta_f}{c} \frac{\partial z_f}{\partial r} + \frac{\sin \theta_f}{c} ,
 \end{aligned}$$

whence

$$\frac{\partial z_f}{\partial r} = - \frac{\beta \sin \theta_f}{1 - \beta \cos \theta_f} \quad (3.27)$$



Similarly, differentiation of Equation 2.8 with respect to  $z$  gives

$$0 = \frac{1}{v} = \frac{\partial z_f}{\partial z} + \frac{1}{c} \frac{(z-z_f) \left(1 - \frac{\partial z_f}{\partial z}\right)}{\sqrt{(z-z_f)^2 + r^2}}$$

$$= \frac{1}{v} \frac{\partial z_f}{\partial z} + \frac{\cos \theta_f}{c} \left(1 - \frac{\partial z_f}{\partial z}\right),$$

whence

$$\frac{\partial z_f}{\partial z} = - \frac{\beta \cos \theta_f}{1 - \beta \cos \theta_f} \quad (3.28)$$

Similarly differentiation of Equation 2.8 with respect to  $t$  gives

$$1 = \frac{1}{v} \frac{\partial z_f}{\partial t} + \frac{1}{c} \frac{(z-z_f) \left(-\frac{\partial z_f}{\partial t}\right)}{\sqrt{(z-z_f)^2 + r^2}}$$

$$= \frac{1}{v} \frac{\partial z_f}{\partial t} - \frac{\cos \theta_f}{c} \frac{\partial z_f}{\partial t},$$

whence

$$\frac{\partial z_f}{\partial t} = \frac{v}{1 - \beta \cos \theta_f} \quad (3.29)$$

It follows from Equation 3.24 that

$$\frac{\partial I}{\partial r} = \frac{\sin \theta}{R(1+\cos \theta)} - \frac{\sin \theta_f}{R_f(1+\cos \theta_f)} - \frac{\beta \sin \theta_f}{R_f(1-\beta \cos \theta_f)} \quad (3.30)$$

Similarly

$$\frac{\partial I}{\partial t} = \frac{v}{R_f(1-\beta \cos \theta_f)} \quad (3.31)$$

and

$$\frac{\partial I}{\partial z} = \frac{1}{R} - \frac{1}{R_f} \left(1 + \frac{\beta \cos \theta_f}{1 - \beta \cos \theta_f}\right) = \frac{1}{R} - \frac{1}{R_f(1-\beta \cos \theta_f)} \quad (3.32)$$

On applying Equations 3.31 to Equation 3.20,

$$H_{\phi} = - \frac{J}{4\pi} \left[ \frac{\sin \theta}{R(1+\cos \theta)} - \frac{\sin \theta_f}{R_f(1+\cos \theta_f)} - \frac{\beta \sin \theta_f}{R_f(1-\beta \cos \theta_f)} \right] \quad (3.33)$$

Similarly, from Equation 3.18

$$\begin{aligned} E_{zm} &= - \frac{J}{4\pi\epsilon_0 v} \left[ \frac{1}{R} - \frac{1}{R_f(1-\beta \cos \theta_f)} + \frac{\beta^2}{R_f(1-\beta \cos \theta_f)} \right] \\ &= - \frac{J}{4\pi\epsilon_0 v} \left[ \frac{1}{R} - \frac{1-\beta^2}{R_f(1-\beta \cos \theta_f)} \right] \end{aligned} \quad (3.34)$$

and from Equation 3.19,

$$E_{rm} = - \frac{J}{4\pi\epsilon_0 v} \left[ \frac{\sin \theta}{R(1+\cos \theta)} - \frac{\sin \theta_f}{R_f(1+\cos \theta_f)} - \frac{\beta \sin \theta_f}{R_f(1-\beta \cos \theta_f)} \right] \quad (3.35)$$

Equations 3.16, 3.17, 3.33, 3.34, and 3.35 constitute the exact formal solution for the fields generated by the charge separation process and the accompanying current flow. The quantities  $R_f$  and  $\theta_f$  may be found in terms of  $z_f$  using Equations 2.7 and 3.22, while  $z_f$  can be found as a function of  $t$  by inverting the time-distance equation (Equation 2.10) as discussed in Appendix A. For numerical calculations it may be expedient to regard  $z_f$  as the independent variable, and to compute the fields and the associated observation time as separate exercises. This approach is illustrated in Section 5.

The above solution gives the fields resolved in a cylindrical coordinate system, that is, they are resolved in the  $r$ ,  $\phi$ , and  $z$ -directions. For completeness the solution will now be re-cast into components appropriate to a spherical coordinate system, that is, in the coordinate directions  $R$ ,  $\theta$ , and  $\phi$ . The  $\phi$ -component (magnetic field) is the same in the two systems, while the others transform in ways that are obvious from inspection of Figure 3.1. Thus

$$E_R = E_z \cos \theta + E_r \sin \theta \quad (3.36)$$

$$E_{\theta} = - E_z \sin \theta + E_r \cos \theta \quad (3.37)$$

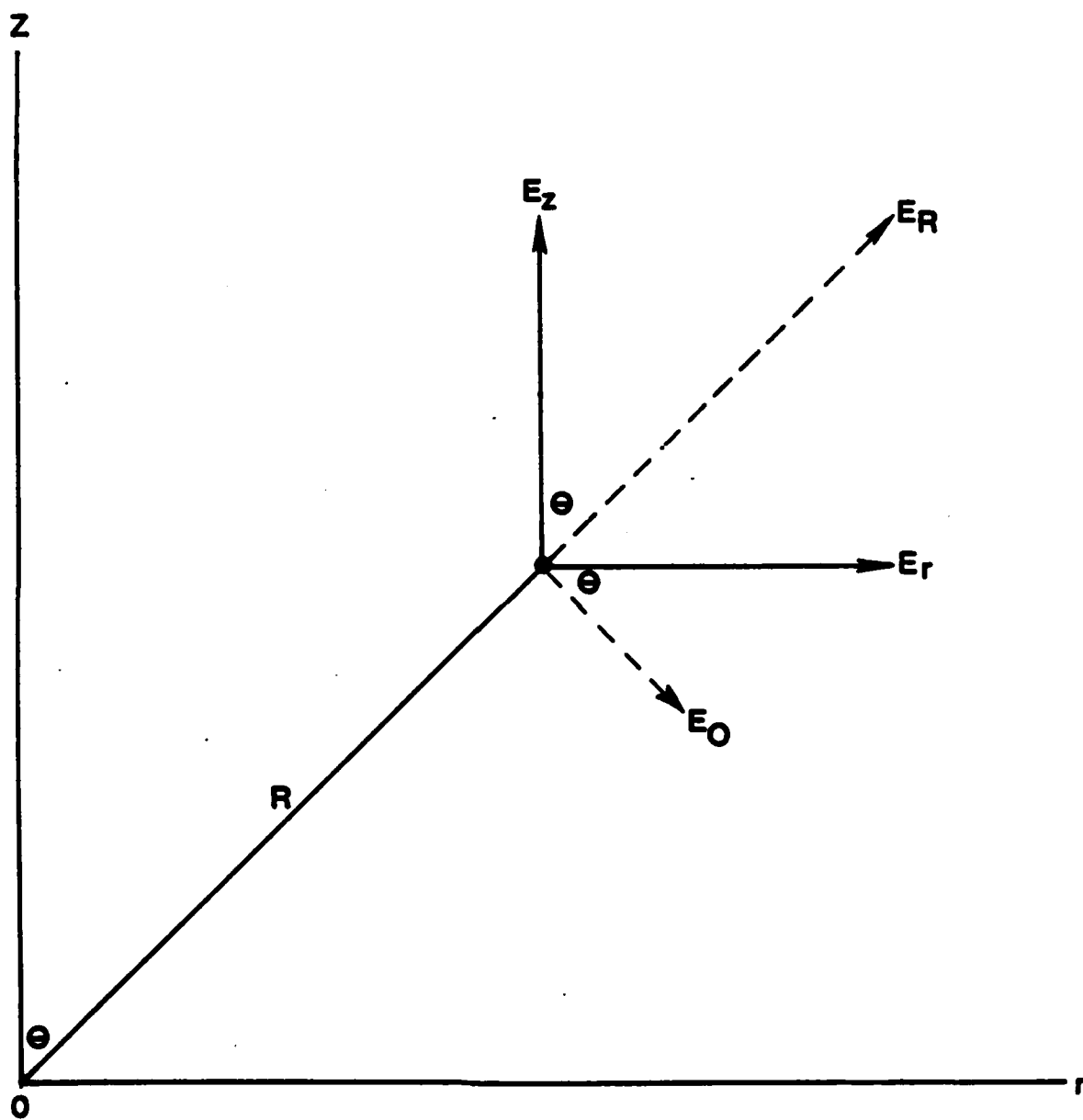


Figure 3.1

Relation of Electric Field-Components in Cylindrical and Spherical Coordinate Systems

Then the fields of the stationary charge, Equations 3.14 and 3.15, appear in spherical components as

$$E_{RS} = - \frac{Jt}{4\pi\epsilon_0 R^2} \quad (3.38)$$

$$E_{\theta S} = 0 \quad (3.39)$$

Similarly, the fields of the moving charge become

$$E_{Rm} = - \frac{J}{4\pi\epsilon_0 v} \left\{ \left[ \frac{1}{R} - \frac{1 - \beta^2}{R_f(1 - \beta \cos \theta_f)} \right] \cos \theta + \left[ \frac{\sin \theta}{R(1 + \cos \theta)} - \frac{\sin \theta_f}{R_f(1 + \cos \theta_f)} - \frac{\beta \sin \theta_f}{R_f(1 - \beta \cos \theta_f)} \right] \sin \theta \right\} \quad (3.40)$$

$$E_{\theta m} = \frac{J}{4\pi\epsilon_0 v} \left\{ \left[ \frac{1}{R} - \frac{1 - \beta^2}{R_f(1 - \beta \cos \theta_f)} \right] \sin \theta - \left[ \frac{\sin \theta}{R(1 + \cos \theta)} - \frac{\sin \theta_f}{R_f(1 + \cos \theta_f)} - \frac{\beta \sin \theta_f}{R_f(1 - \beta \cos \theta_f)} \right] \cos \theta \right\} \\ = \frac{J}{4\pi\epsilon_0 v} \left\{ \left[ \frac{\cos \theta}{R(1 + \cos \theta)} - \frac{1 - \beta^2}{R_f(1 - \beta \cos \theta_f)} \right] \sin \theta + \left[ \frac{1}{R_f(1 + \cos \theta_f)} + \frac{\beta}{R_f(1 - \beta \cos \theta_f)} \right] \sin \theta_f \cos \theta \right\} \quad (3.41)$$

#### 4. LIMITING FORMS FOR LARGE DISTANCES AND EARLY TIMES

If  $R$  is large and  $z_f$  is small, a situation which may occur when the current-front has not yet moved far from the origin, some simplified limiting forms can be obtained. Thus

$$R_f \rightarrow R \quad (4.1)$$

$$\theta_f \rightarrow \theta \quad (4.2)$$

and from Equation 3.24,

$$H_\phi \rightarrow \frac{J}{4\pi R} \cdot \frac{\beta \sin\theta}{1 - \beta \cos\theta} \quad (4.3)$$

and by Equation 3.27,

$$E_{\theta m} \rightarrow \frac{JZ_o}{4\pi R} \cdot \frac{\sin\theta}{1 - \beta \cos\theta} \quad (4.4)$$

Using Equation 3.25,

$$E_{zm} \rightarrow \frac{J}{4\pi\epsilon_o cR} \cdot \frac{\cos\theta - \beta}{1 - \beta \cos\theta} \quad (4.5)$$

In spherical coordinates, the radial component simplifies immediately:

$$E_{Rm} \rightarrow \frac{J}{4\pi\epsilon_o cR} = \frac{JZ_o}{4\pi R} \quad (4.6)$$

while

$$E_{\theta m} \rightarrow \frac{J}{4\pi\epsilon_o cR} \cdot \frac{\beta \sin\theta}{1 - \beta \cos\theta} = Z_o H_\phi \quad (4.7)$$

Also at early times

$$t \rightarrow \frac{R}{c} \quad (4.8)$$

and by Equation 3.30,

$$E_{RS} \rightarrow - \frac{J}{4\pi\epsilon_0 cR} \quad (4.9)$$

so that

$$E_R = E_{RS} + E_{Rm} \rightarrow 0$$

Since  $E_{\theta S} = 0$  (see Equation 3.31),

$$E_{\theta} = E_{\theta m} \rightarrow Z_0 H_{\phi} \quad (4.10)$$

To summarize these limiting forms, valid for large distances and early times, it is concluded that (a) the radial or R-field of the moving charge cancels the field of the stationary charge giving no net radial field, (b) the tangential electric field and the azimuthal magnetic field are related to each other as in a plane wave, or as in the far field of an oscillating infinitesimal dipole, (c) the directional pattern differs from that of an infinitesimal dipole by the factor

$$\gamma = \frac{1}{1 - \beta \cos \theta} \quad (4.11)$$

This factor can produce a very large effect if  $\beta$  is close to unity, but the effect is small if  $\beta$  is small. In any case  $\gamma=1$  at  $\theta = 90^\circ$ . Figure 4.1 illustrates the behaviour of the directional pattern

$$F(\theta, \beta) = \frac{\beta \sin \theta}{1 - \beta \cos \theta} \quad (4.12)$$

for two values of  $\beta$ .

(d) The radiation fields are maximum in the cone of directions for which

$$\theta = \cos^{-1} \beta \quad (4.13)$$

and

$$F = \frac{\beta}{\sqrt{1 - \beta^2}} \quad (4.14)$$

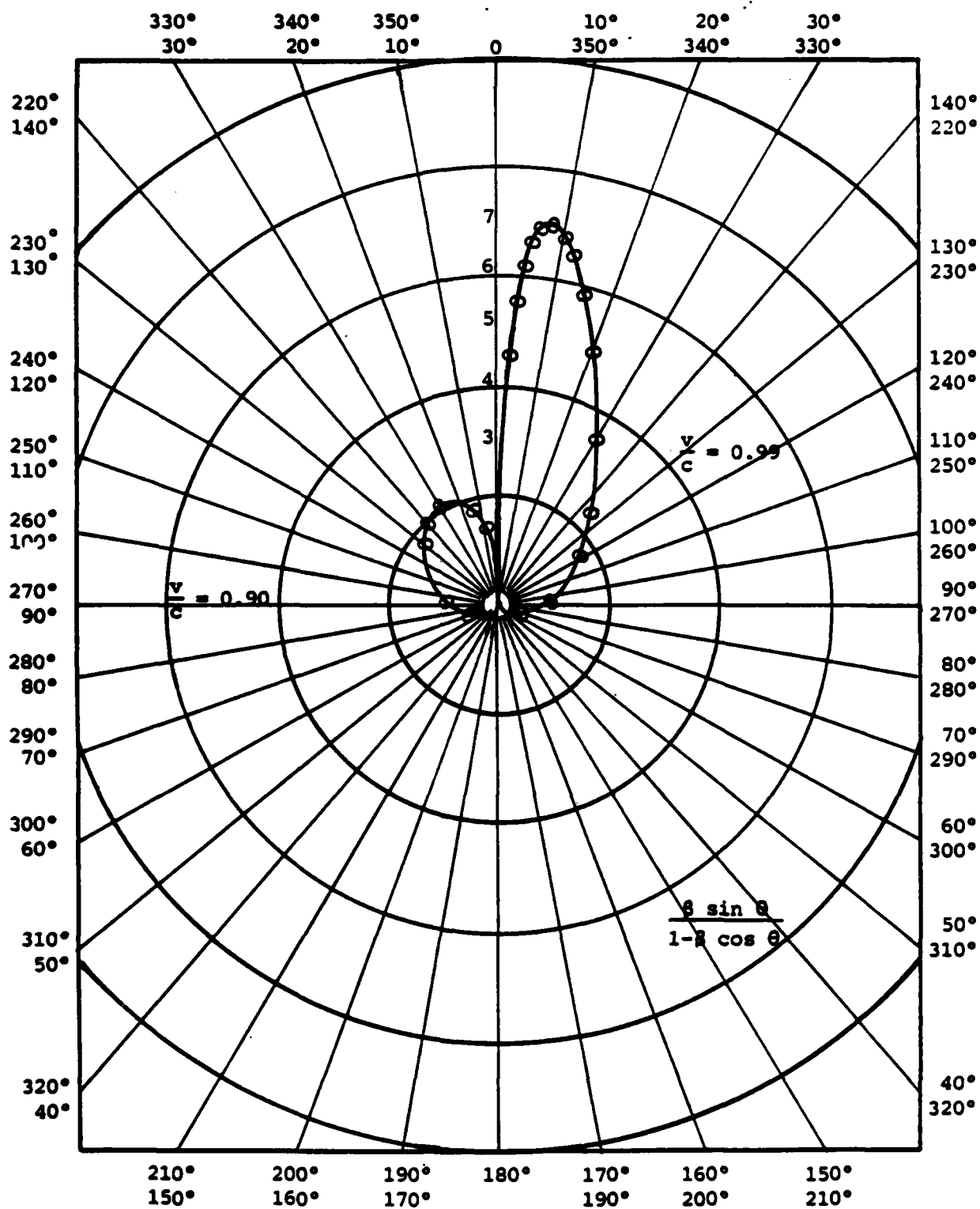


Figure 4.1

Directivity Patterns for Early Times

(e) Like the stepfunction of the source current itself, these limiting forms for large distances have sudden onsets, and constant amplitudes.

The radiated power may be found by considering the electromagnetic energy density between two expanding wavefronts at a large distance from the origin. Figure 4.2 illustrates the positions of two spherical wavefronts at time  $t$ . The outer wavefront started from the origin  $O$  at time zero, and hence is at a radius  $R = ct$ . The inner wavefront was radiated from point  $A$ , at a time

$\Delta t = \frac{\overline{OA}}{v}$  later, and hence appears at radius

$$R_A = c(t - \Delta t) = R - c\Delta t \quad (4.15)$$

It may be seen from Figure 4.2 that the width  $\Delta$  of the space between the wavefronts in the  $\theta$ -direction is given approximately by

$$\Delta W \approx R - R_A - \overline{OA} \cos \theta \quad (4.16)$$

and in the limit,

$$dW = cdt - vdt \cos \theta = (1 - \beta \cos \theta) cdt \quad (4.17)$$

Now if the volume density of electromagnetic energy is taken to be

$$\mathcal{E} = \frac{1}{2} \epsilon_0 E^2 + \frac{1}{2} \mu_0 H^2 \quad \text{joules m}^{-3} \quad (4.18)$$

(See Stratton, 2 p. 111, Equation (32), and p. 124, Equation (34)) it follows from Equation 4.10 that

$$\mathcal{E} = \left( \frac{1}{2} \epsilon_0 \dot{z}_o^2 + \frac{1}{2} \mu_0 \right) H_\phi^2 = \mu_0 H_\phi^2 \quad (4.19)$$

$$= \frac{j^2 \mu_0}{16\pi^2 R^2} \cdot \frac{\beta^2 \sin^2 \theta}{(1 - \beta \cos \theta)^2} \quad (4.20)$$

by Equation 4.3.



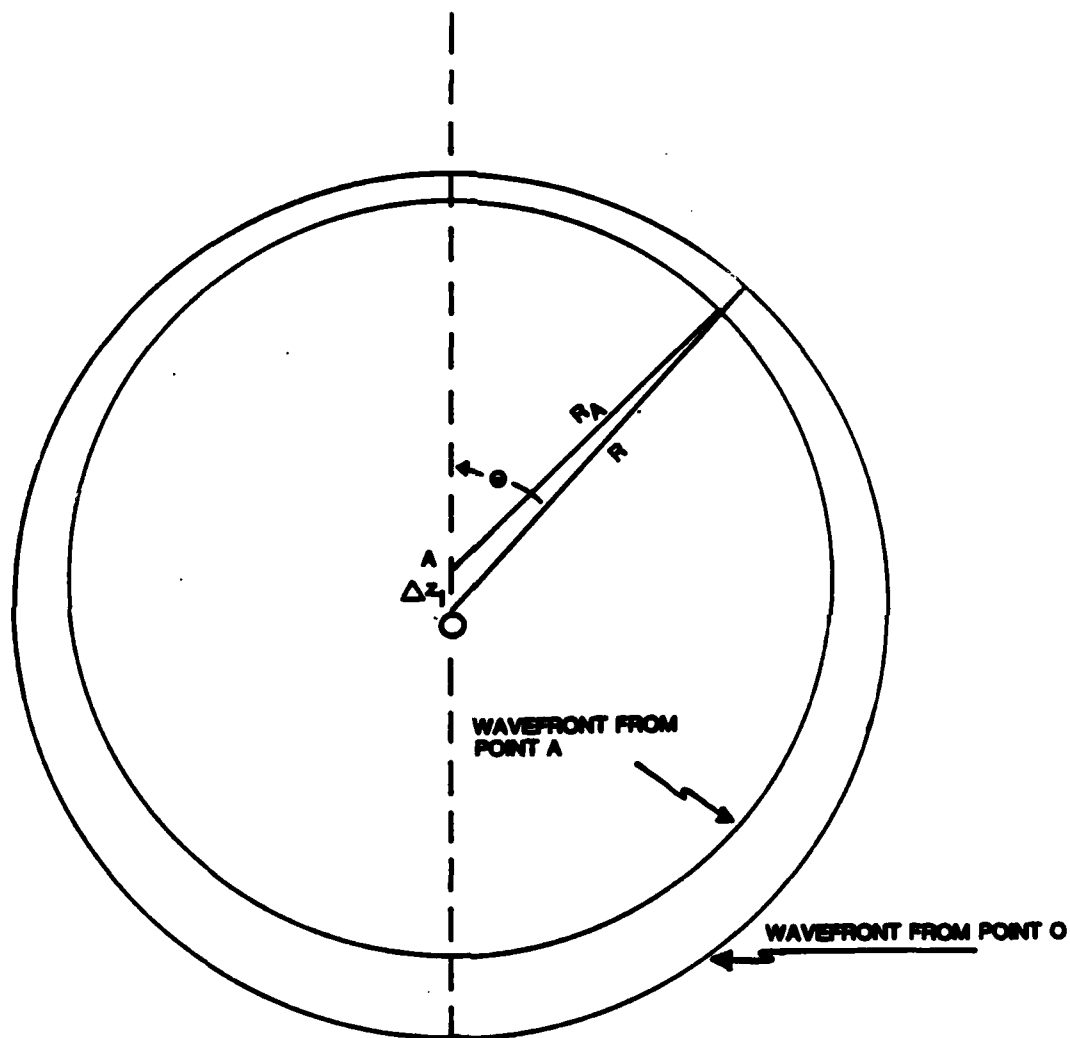


Figure 4.2  
 Cross-section of the Space Between Two Neighboring Wavefronts

The energy  $du$  between the wavefronts is found by integration using an elemental volume illustrated in Figure 4.3. The element is a ring of radius  $R \sin \theta$ , and a crosssectional area  $R d\theta dW$ , and volume

$$\begin{aligned} dv &= R^2 \sin \theta d\theta dW \\ &= cR^2 \sin \theta \cdot (1 - \beta \cos \theta) dt d\theta \end{aligned} \quad (4.21)$$

Then

$$\begin{aligned} du &= \int_{\text{volume}} \mathcal{E} dv \\ &= \frac{J^2 \mu_0 c dt}{16\pi^2} \cdot B(\beta) \end{aligned} \quad (4.22)$$

where

$$B(\beta) = \beta^2 \int_0^\pi \frac{\sin^3 \theta}{1 - \beta \cos \theta} d\theta \quad (4.23)$$

$$= \beta^2 \int_{-1}^{+1} \frac{1 - \alpha^2}{1 - \beta \alpha} d\alpha \quad (4.24)$$

This integral is readily evaluated using standard forms, (for example Dwight<sup>3</sup> Items 90.1 and 92.1) and after some algebraic reduction it is found that

$$B(\beta) = 2 - \left(\frac{1}{\beta} - \beta\right) \ln \frac{1 + \beta}{1 - \beta} \quad (4.25)$$

The function  $B(\beta)$  is illustrated in Figure 4.4: it varies from 0 to 2 and varies from 0 to 1.

Since the energy  $du$  was radiated in time  $dt$ , the radiated power was

$$\frac{dU}{dt} = J^2 \frac{Z_0 B(\beta)}{16\pi^2} \quad (4.26)$$

<sup>3</sup> Dwight, H.B., "Tables of Integrals and Other Mathematical Data", MacMillan, 1943.

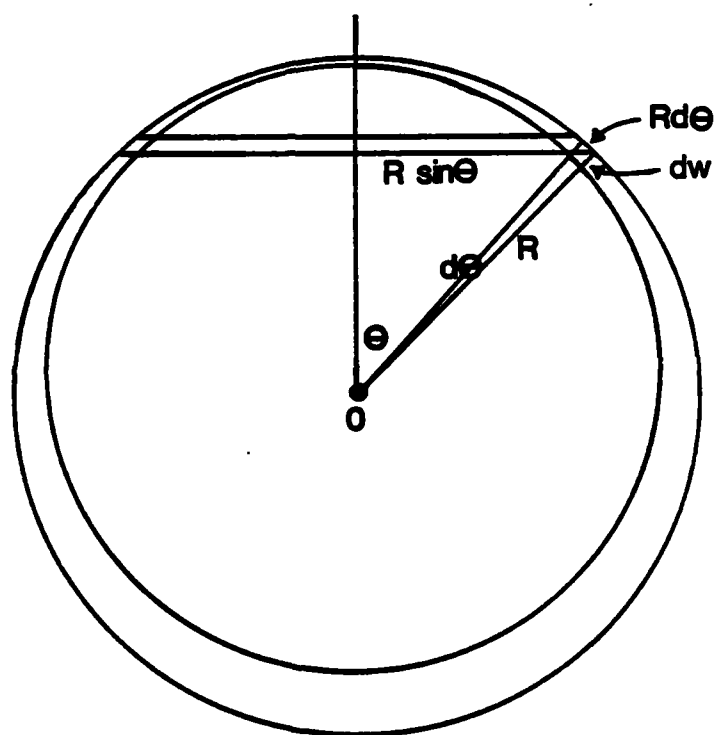


Figure 4.3  
Element of Integration

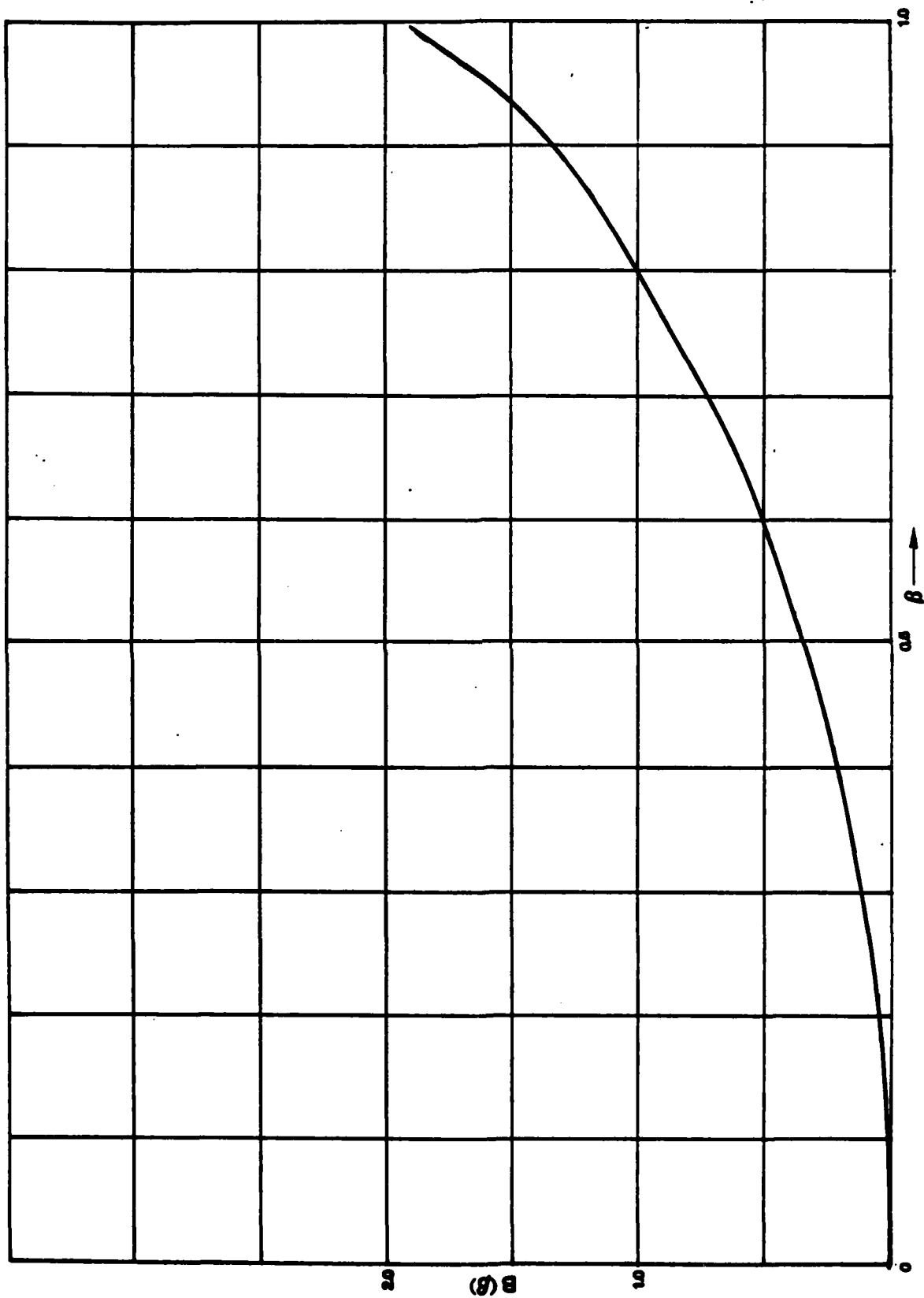


Figure 4.4  
Graph of the Function  $B(\beta)$

The power radiated is evidently equivalent to the power that would be expended if the current  $J$  were flowing in a "radiation resistance"

$$R = \frac{Z_0 B}{16\pi^2} \quad (4.27)$$

Since  $B$  has the maximum value of 2, the maximum value of  $R$  is 4.7746 ohms.

The preceding results for a step-function current transient can be used to calculate the fields from an arbitrary current-transient propagating along a straight line without change of amplitude or shape. Such a transient can be considered to consist of a linear superposition of elemental step-functions, and it follows that the early-time and large-distance radiation waveforms resemble the waveform of the current when displayed on appropriate amplitude and time scales. For example, a current impulse in the form of a delta-function can be modelled by a positive step-function followed, after a short delay  $\Delta t$ , by an equal but negative current-step. The latter in effect cancels the former after a current-impulse  $\Delta t J = q$  is delivered. The duration of the fields is also  $\Delta t$ , and the field impulses follow immediately from Equation 4.7:

$$\int E_{\theta m} dt = Z_0 \int H_{\phi} dt = \frac{q}{4\pi\epsilon_0 c R} \cdot \frac{\beta \sin\theta}{1 - \beta \cos\theta} \quad \text{volt} \cdot \text{sec} \cdot \text{m}^{-1} \quad (4.28)$$

## 5. NUMERICAL EXAMPLE

In certain practical cases it may not suffice to consider only early times, or only fields varying as  $1/R$ , as was done in Section 4. In those cases it may be expedient to resort to numerical work with machine computation. In this Section fields are calculated for the following numerical example

$$R = 1 \text{ m}$$

$$J = 1 \text{ amp}$$

$$\beta = 0.99$$

$$\cos\theta = 0.99$$

$$(\theta \approx 8.1096^\circ)$$

$$z = \cos\theta = 0.99$$

$$r = \sin\theta = 0.141067$$

(5.1)

Then by Equation 2.7,

$$R_f = \sqrt{1 - 1.98z_f + z_f^2} \quad , \quad (5.2)$$

and by Equation 3.22,

$$\cos\theta_f = \frac{0.99 - z_f}{R_f} \quad (5.3)$$

Also, by Equation 3.23,

$$\sin\theta_f = \frac{0.14106}{R_f} \quad (5.4)$$

From Equation 2.8,

$$t = \frac{1}{c} \left( \frac{z_f}{\beta} + R_f \right) \quad (5.5)$$

where  $c = 3 \times 10^8$  m/s. The first fields arrive at time  $t = 3.33333$  ns.

Equation 3.33 reduces to

$$H_\phi = - \frac{1}{4\pi} \left[ 0.70881 - \frac{0.28071}{R_f^2} \cdot \frac{1}{(1+\cos\theta_f)(1-\beta\cos\theta_f)} \right] \text{ amp/m} \quad (5.6)$$

While by Equation 3.21

$$E_{rm} = 380.799H_\phi \quad \text{v/m} \quad (5.7)$$

If  $t_{ns}$  is time in nanoseconds, Equation 3.17 gives

$$E_{rs} = - 1.2678t_{ns} \quad \text{v/m} \quad (5.8)$$

$$E_r = 380.799H_\phi - 1.2678t_{ns} \quad (5.9)$$

By Equation 3.16, similarly,

$$E_{zs} = - 8.9100t_{ns} \quad \text{v/m} \quad (5.10)$$

Finally, by Equation 3.34

$$E_{zm} = -30.3030 + \frac{0.20101}{R_f - 0.9801 + 0.99z_f} \quad (5.11)$$

and

$$E_z = E_{zs} + E_{zm} \quad (5.12)$$

By assuming various values of  $z_f$ , the corresponding values of  $t$ ,  $R_f$ , and  $\cos$  were found. With these, values of the fields were calculated, and the results are sketched in Figures 5.1, 5.2, and 5.3. It may be noted that the shoulders of the curves are definitely rounded, whereas it was seen in the previous Section that the early-time far-fields have abrupt (discontinuous) onsets.

## 6. CURRENT GENERATION AND ABSORPTION

In the previous Sections the travelling current-front was assumed to continue along a line indefinitely, but in some cases of interest the model should provide for stopping, and even reversing, the current at an arbitrary point. For example, a current wave on a conductor of finite length must stop or reverse when the end is reached. These cases can be treated by linear superposition of solutions of the basic model already discussed. For example, the advance of the current front can in effect be stopped at a point by starting a new current at that point. The current travels in the same direction but has opposite sign so as to cancel the original current. Similarly, a current reversal can be modelled by stopping the original current as just described, and generating a third current having the same sign as the original one, but travelling in the reverse direction.

The case of stopping the current will be considered in more detail. It will be assumed as before that the current step is generated at the origin of coordinates but now when the front reaches the point  $z = L$ , see Figure 6.1, the new current begins. This (negative) current leaves an increasing positive charge at  $z = L$ , and this is of course equivalent to the positive charge that would accumulate when the original current is stopped. The original current front reaches the point  $z = L$  at time  $L/v$ , and the effects of this arrival reach the observer at time

$$t_L = \frac{L}{v} + \frac{R_L}{c} \quad (6.1)$$

where

$$R_L = \sqrt{(z-L)^2 + r^2} \quad (6.2)$$

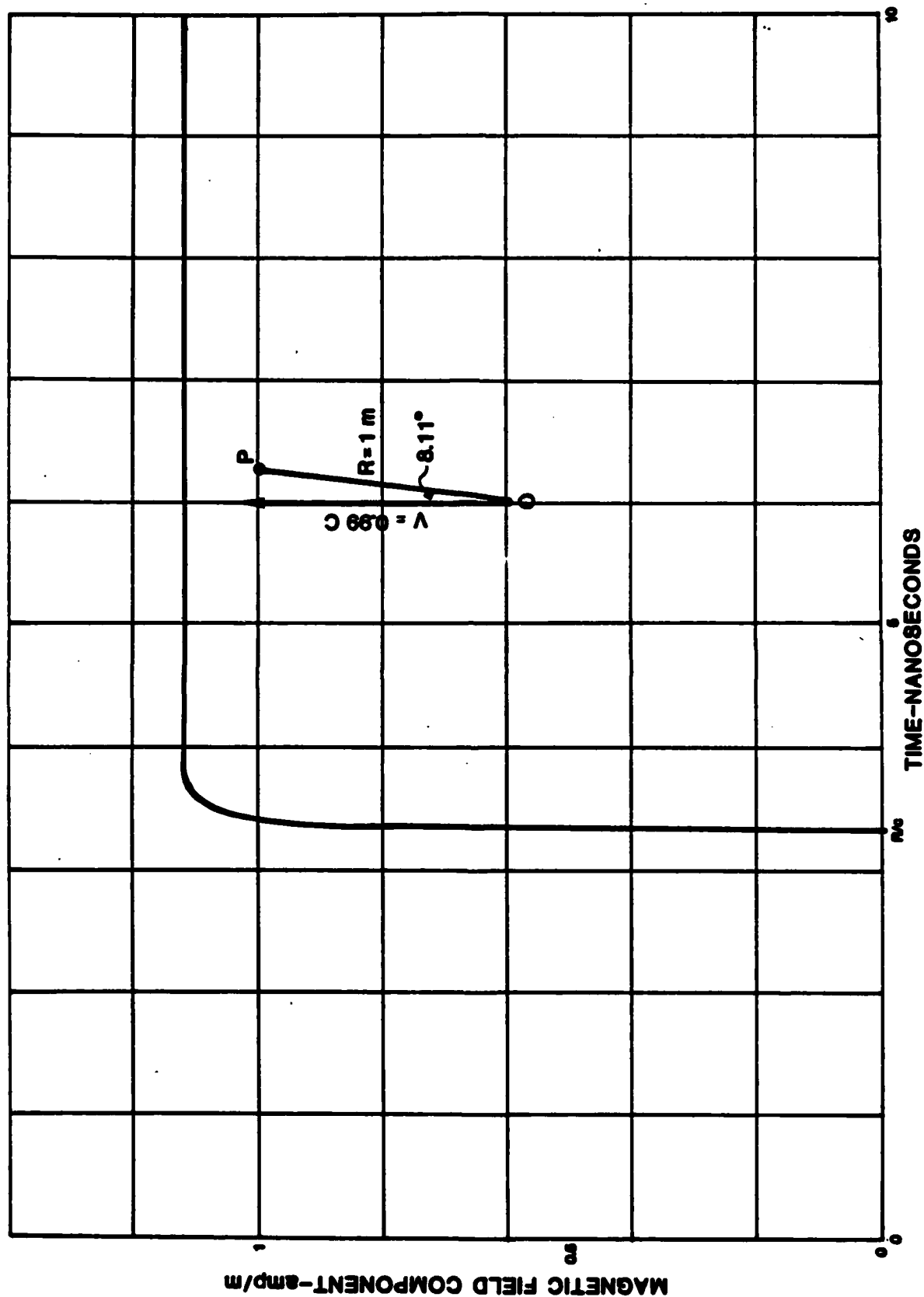


Figure 5.1

Growth of Magnetic Field  $H_\phi$  From Equation 5.6



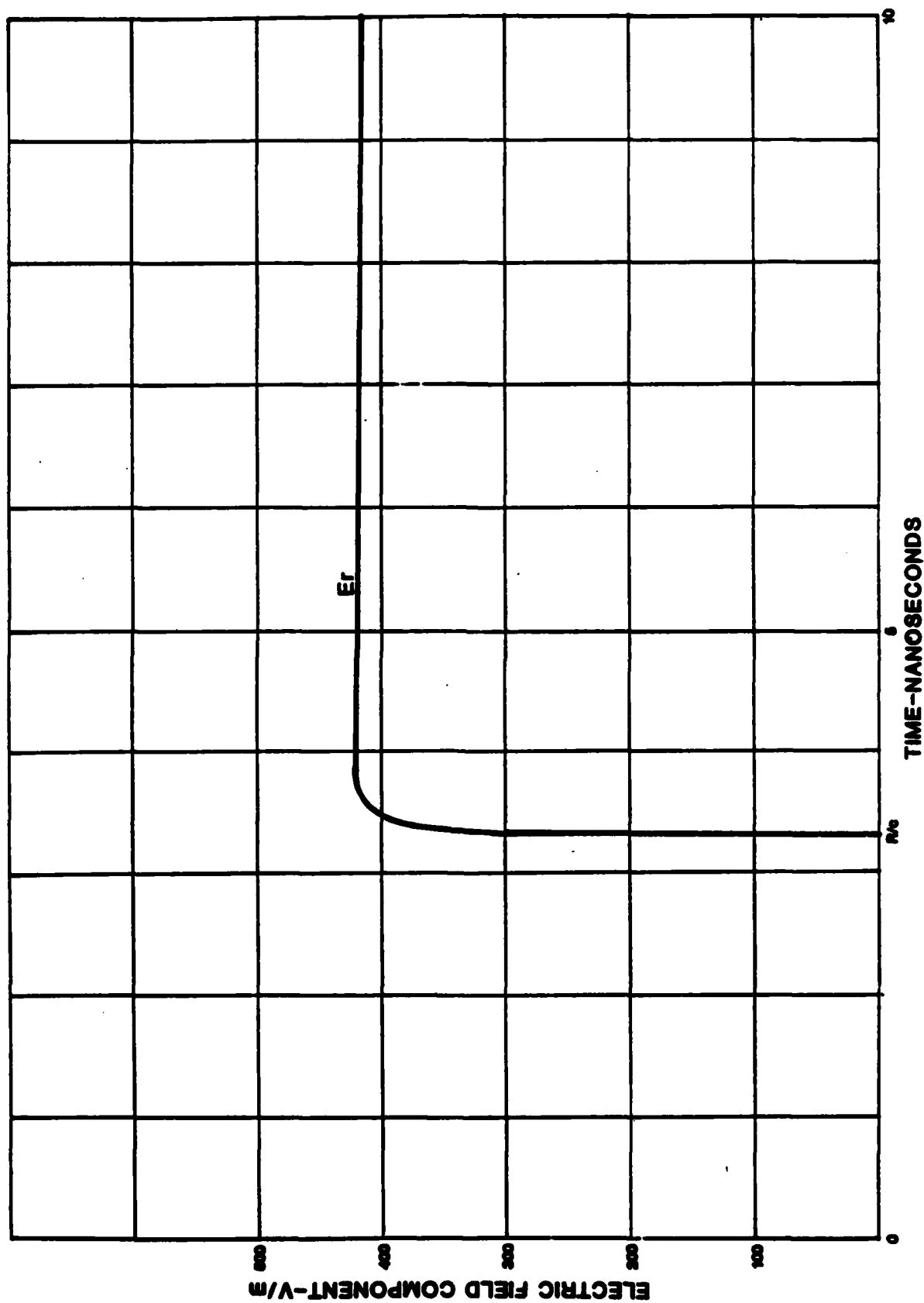


Figure 5.2

Growth of the Electric Field Component  $E_p$  From Equation 5.9

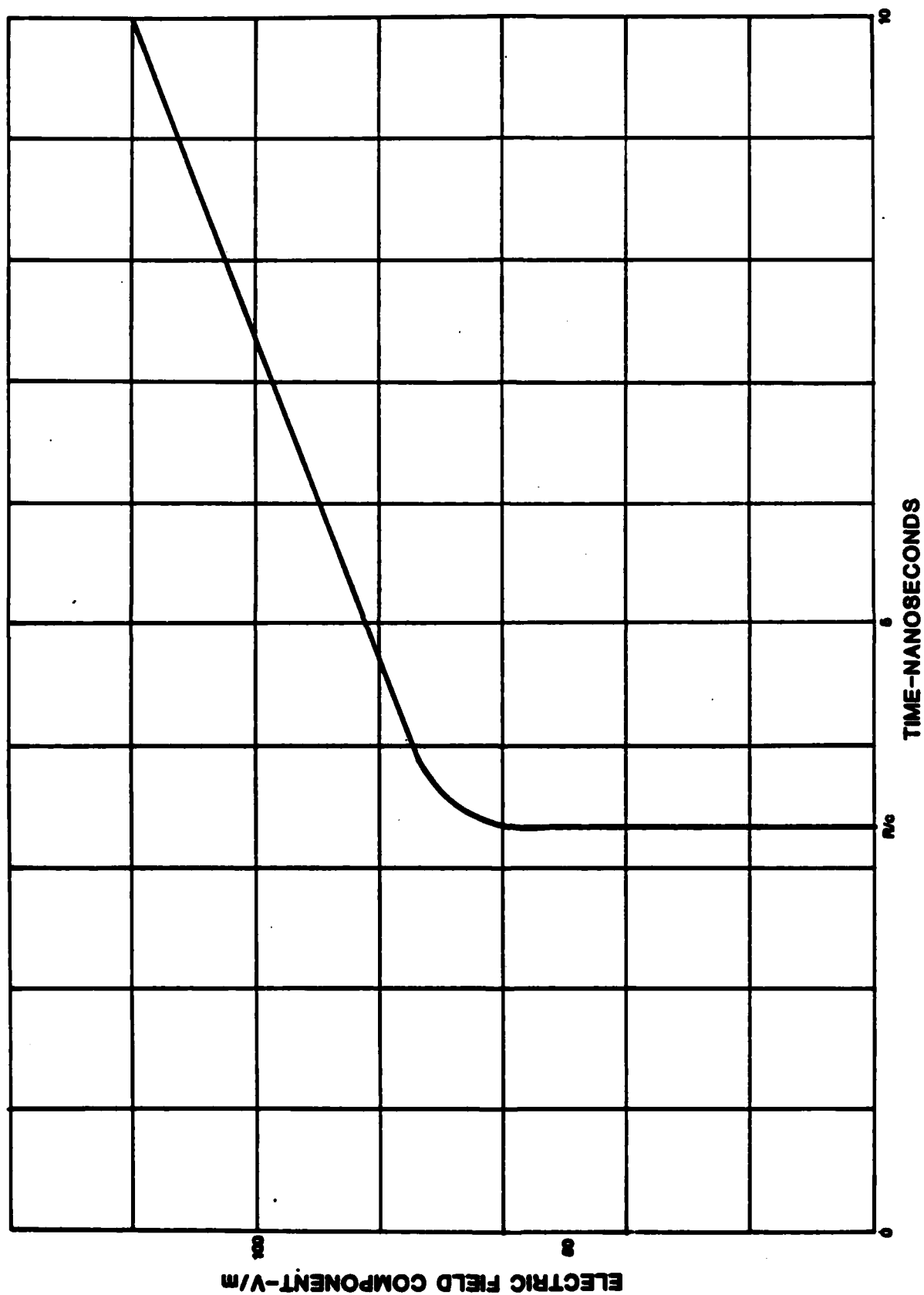


Figure 5.3  
Growth of the Electric Field Component  $E_z$  From Equation 5.12

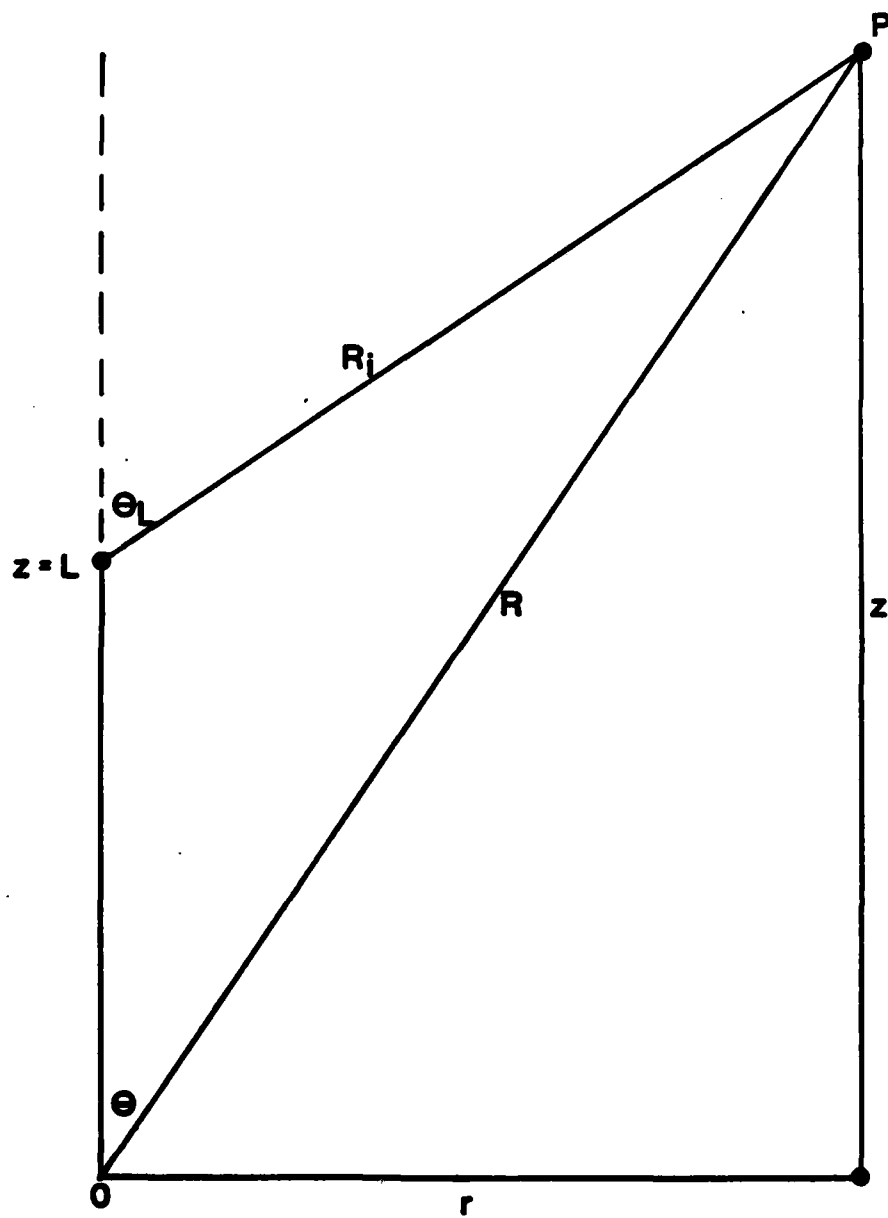


Figure 6.1

Version of Figure 2.1 for the Case when the Upward-Advancing  
Current-Front is Absorbed at  $z=L$

Prior to that instant the fields at the observer are exactly the same as in the previous case. After that instant the new fields must be added. The latter can be calculated using the previous formulas, except that the origin of coordinates for the new fields is at  $z = L$ , and not at  $z = 0$ .

Whereas the fields are readily calculated, formally combining the various expressions is rather cumbersome except in the limiting case when  $R$  and  $R_L$  are large. This special case is discussed in Section 7.

## 7. LIMITING FORMS WITH CURRENT ABSORPTION

Figure 7-1(a) is an amplitude-time representation of the radiation-field waveform at a great distance, caused by the generation and absorption of a positive current-step. The field lasts for a time  $\Delta t_L$  given by Equation 7.4. Figure 7-1(b) illustrates the radiation waveform of a negative current step of the same amplitude, but delayed a short time  $\Delta t$  from the positive step. Figure 7-1(c) illustrates the linear combination of the two previous waveforms, and hence represents the radiation waveform of a current impulse. It is seen that the radiation waveform consists of two impulses—a prompt impulse, followed by a delayed impulse of opposite sign. Since any arbitrary current waveform can be considered to be made up of a sequence of current impulses of suitable amplitudes, the corresponding radiation waveform is followed by a similar but inverted and delayed waveform, beginning after the time  $\Delta t_L$ . Thus if Figure 7-2(a) represents the waveform from generating the current, then Figure 7-2(c) represents the composite radiation waveform.

The radiation field due to the generation of the arbitrary current  $I(t)$  is proportional to  $I(t - \frac{R}{c})$ , while the "absorption field" is proportional to  $-I(t - \frac{R}{c} - \Delta t_L)$

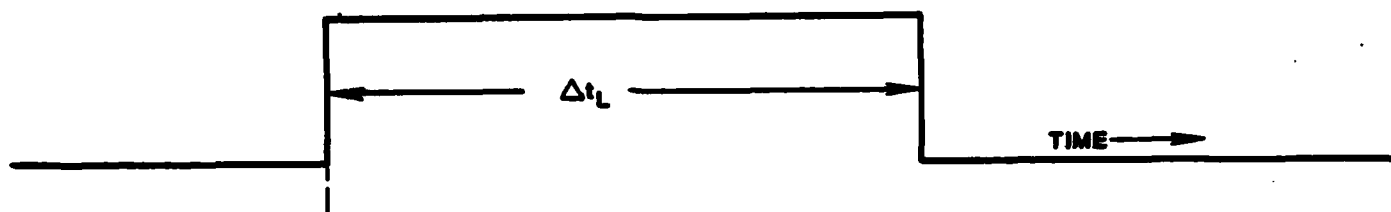
Thus the composite field is proportional to

$$\frac{I(t - \frac{R}{c}) - I(t - \frac{R}{c} - \Delta t_L)}{\Delta t_L} \cdot \Delta t_L \quad (7.1)$$

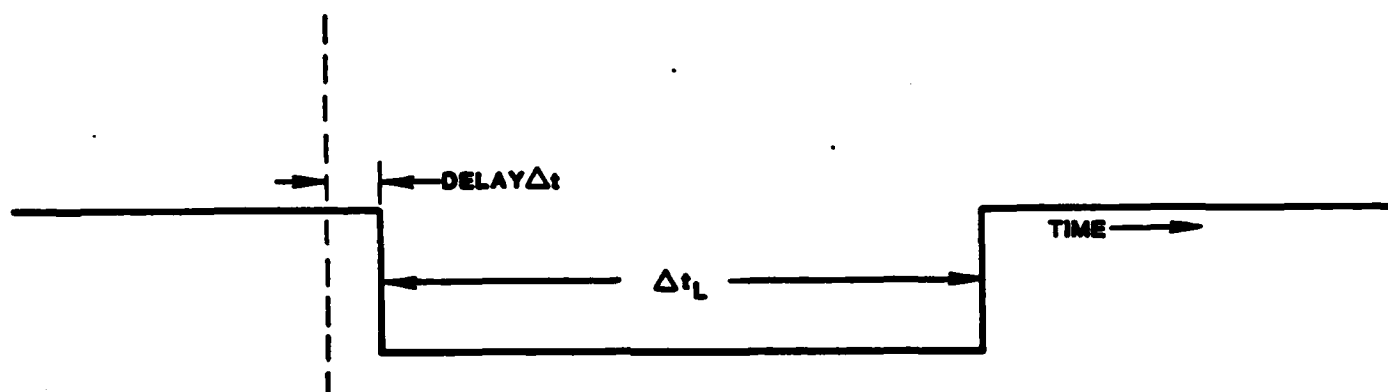
and hence to

$$\frac{L}{v} \cdot \frac{dI(t - \frac{R}{c})}{dt} \quad (7.2)$$

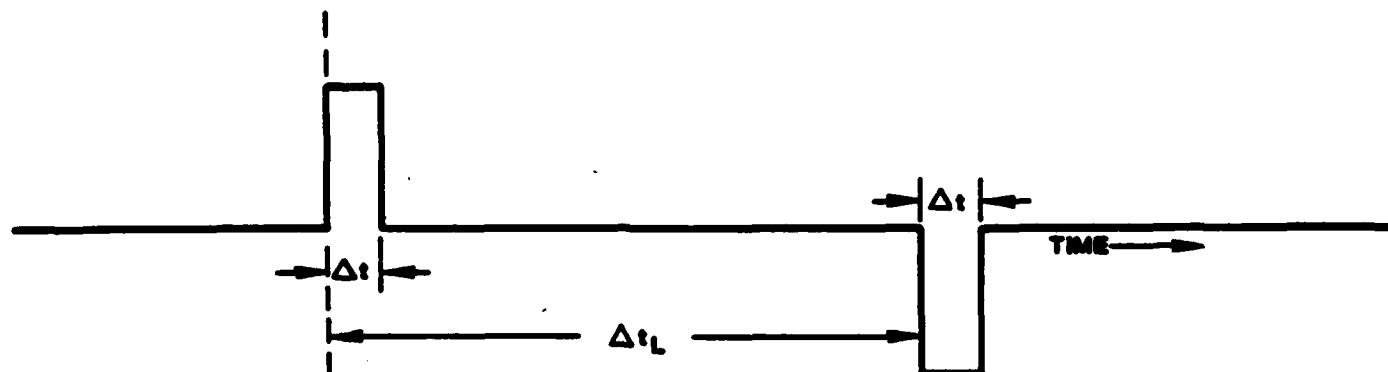
when  $L$  and  $v/c$  are small. This proportionality of the radiation field to length times rate-of-change of current is a well known result with conventional infinitesimal dipole radiators.



(a) Radiation Waveform From Generating and Absorbing a Positive Current Step



(b) Radiation Waveform From Generating and Absorbing a Delayed Negative Current Step



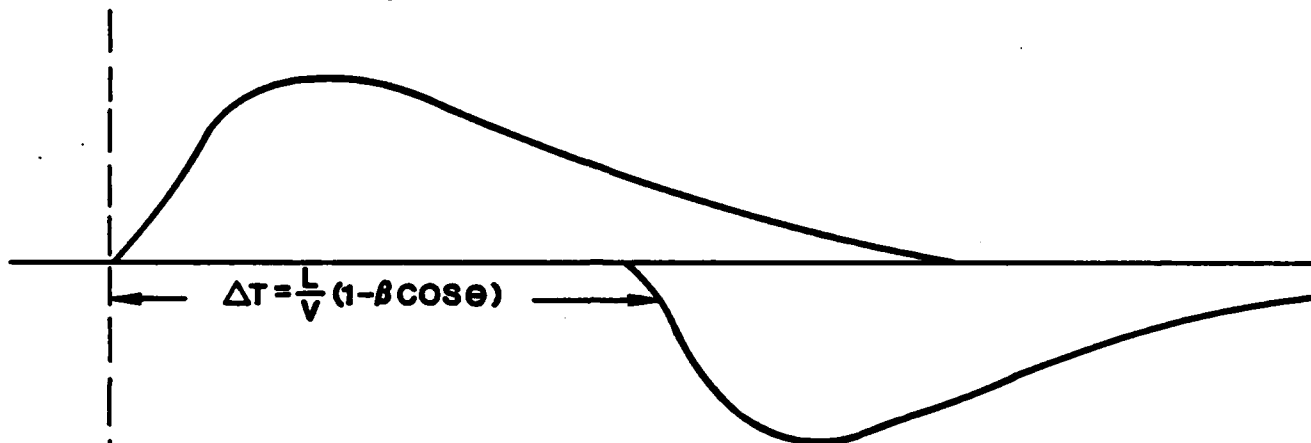
(c) Composite Radiation Waveform

Figure 7.1

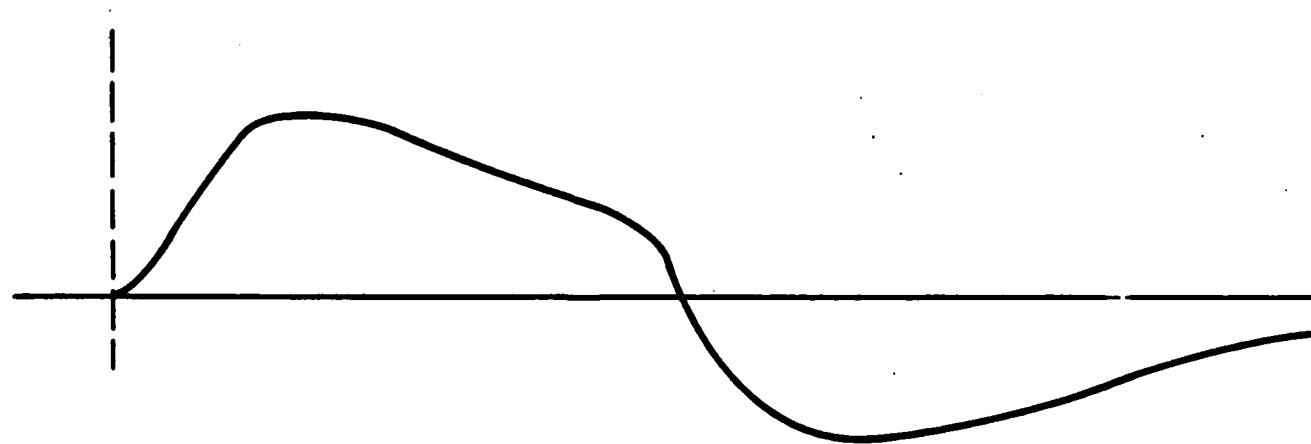
Generating and Absorbing a Current Impulse Gives a  
Double-Impulse Radiation Field



(a) Illustrative Radiation Waveform From Generating an Arbitrary Current



(b) Corresponding Radiation Waveform From Absorbing the Current



(c) Composite Radiation Field

Figure 7.2

Synthesis of Radiation Field From Generating and Absorbing an Arbitrary Current

## Appendix A:

### Inversion of the Time-Distance Equation

On writing the time-distance relation, Equation 2.8, as

$$vt - z_f = \beta \sqrt{(z - z_f)^2 + r^2} \quad (\text{A.1})$$

with  $\beta = v/c$ , squaring both sides gives

$$v^2 t^2 - 2vtz_f + z_f^2 = \beta^2 (z^2 - 2zz_f + z_f^2 + r^2) \quad (\text{A.2})$$

This when re-arranged reads

$$(1 - \beta^2)z_f^2 - 2Pz_f + Q = 0 \quad , \quad (\text{A.3})$$

where

$$P = vt - \beta^2 z \quad , \quad (\text{A.4})$$

$$Q = v^2 t^2 - \beta^2 z^2 - \beta^2 r^2 \quad (\text{A.5})$$

There are two solutions to the quadratic Equation A-3, namely

$$z_f = \frac{P \pm \sqrt{P^2 - (1 - \beta^2)Q}}{1 - \beta^2} \quad (\text{A.6})$$

To select the physically significant root, it is noted that with  $t = R/c$ , the quantity  $Q = 0$ . For equation A-6 to give the correct value  $z_f = 0$  for that case, it is evidently necessary to choose the negative sign.

## REFERENCES

- 1 Lewis, E.A., "Radiation from Idealized Shock Excitation Currents in a Straight Conductor Rising from a Perfect Earth at an Arbitrary Angle" Electromagnetic Wave Propagation, Academic Press, 1958, p335.
- 2 Stratton, J.A. Electromagnetic Theory, McGraw-Hill, 1941.
- 3 Dwight, H.B., "Tables of Integrals and Other Mathematical Data", MacMillan, 1945.





## *MISSION of Rome Air Development Center*

*RADC plans and executes research, development, test and selected acquisition programs in support of Command, Control Communications and Intelligence (C<sup>3</sup>I) activities. Technical and engineering support within areas of technical competence is provided to ESD Program Offices (POs) and other ESD elements. The principal technical mission areas are communications, electromagnetic guidance and control, surveillance of ground and aerospace objects, intelligence data collection and handling, information system technology, ionospheric propagation, solid state sciences, microwave physics and electronic reliability, maintainability and compatibility.*

**END**

**FILMED**

**12-84**

**DTIC**